ISBN: 978-3-95450-261-5 ISSN: 2673-7000 doi: 10.18429/JACoW-NAPAC2025-TUP075

# OPTIMIZING 4D EMITTANCE MEASUREMENTS USING THE PINHOLE SCAN TECHNIQUE

P. P. Owusu[†,1], C. Zhang[2], A. Bartnik[2], T. Kalpada[1], J. Anawalt[1], J. Maxson[2], S. Karkare[1]
[1]Arizona State University, Tempe, AZ, USA
[2]Cornell University, Ithaca, NY, USA

*Abstract*

Accurate measurement of electron beam emittance is essential for optimizing high-brightness electron sources. The Pinhole Scan Technique measures the 4D phase space and hence the emittance by measuring the beam profile after clipping the beam using a pinhole followed by a drift section and then scanning the beam over the pinhole. This technique has been implemented in low energy (< 200 keV) beamlines at both Cornell University and Arizona State University. However, the technique poses several practical challenges. In this work, we analyze and address key issues affecting the 4D phase space and emittance measurements using this technique. We identify and investigate sources of inaccuracies like the pinhole aspect ratio, beam divergence, position-momentum correlations in the phase space, and the point-spread-function of the detector and suggest techniques to minimize them. Our findings offer a pathway to more accurate 4D phase space characterization in advanced electron beam systems.

## INTRODUCTION

A general figure of merit for electron beam quality is its transverse emittance, which characterizes its phase-space distribution. Precise emittance measurement and characterization of the 4D transvserse phase space of electron beams is thus vital for the refinement of electron sources in high-brightness applications. The pinhole scan technique is a powerful tool for characterizing the full 4D phase space of electron beams and obtaining the emittance. This technique has been implemented in the Cornell MEDUSA Beamline, the Cornell Photocathode Lab [1] and the ASU CryoGun Beamline [2, 3]. In this method, a small, precisely defined aperture (or "pinhole") is placed in the path of a focused electron beam to spatially select a tiny portion of the beam. The beam is then systematically scanned across this pinhole by varying the transverse beam position using dipole steering magnets. For each position of the beam relative to the pinhole, the transmitted electrons form a beamlet that travels through a drift space. The transverse distribution of this beamlet is recorded on a downstream detector, typically a scintillator screen coupled to a high-resolution camera. This transverse distribution represents the transverse momentum distribution in the beamlet. By collecting a series of these transmitted beamlet images as the beam is rastered across the aperture in both transverse directions, a detailed map of the beam's four-dimensional transverse phase space $(x, x', y, y')$ can be reconstructed. Here, $x$ and $y$ represent the transverse spatial coordinates at the aperture plane, while $x'$ and $y'$ correspond to the transverse angles (or momenta) derived from the positions on the detector and the known drift length. This dataset allows for the calculation of the full four-dimensional beam covariance matrix as below:

$$\Sigma_{4D} = \begin{bmatrix} \langle xx \rangle & \langle xx' \rangle & \langle xy \rangle & \langle xy' \rangle \\ \langle x'x \rangle & \langle x'x' \rangle & \langle x'y \rangle & \langle x'y' \rangle \\ \langle yx \rangle & \langle yx' \rangle & \langle yy \rangle & \langle yy' \rangle \\ \langle y'x \rangle & \langle y'x' \rangle & \langle y'y \rangle & \langle y'y' \rangle \end{bmatrix} \quad (1)$$

from which the beam's 4D normalized transverse emittance is computed as:

$$\epsilon_{4D,n} = (\gamma\beta)^2 \sqrt{\det(\Sigma_{4D})} \quad (2)$$

where $\gamma$ is the Lorentz factor, $\beta = v/c$, and $\det(\Sigma_{4D})$ is the determinant of the 4D beam matrix [1].

This method measures the full 4D phase space and captures correlations between transverse planes revealing subtle beam distortions caused by aberrations or space charge effects that degrade beam performance making it particularly useful for precise characterization and optimization of the electron beam.

Assuming the normalized transverse emittance is invariant in the beamline, it can then be used to extract the mean transverse energy (MTE) of the electrons emitted from the photocathode through the relation:

$$\text{MTE} = \frac{\epsilon_{4D,n}}{\sigma_i^2 m_0 c^2} \quad (3)$$

In this expression, $\sigma_i$ is the RMS laser spot size at the photocathode, and $m_0c^2$ is the rest mass energy of the electron [2].

Despite its advantages, the pinhole scan technique presents inherent challenges that affect the accuracy of the emittance values obtained. In this work, we identify the key issues related to the pinhole aspect ratio, beam divergence, position-momentum correlations in the phase space, and the point-spread-function of the detector. We also outline the steps taken to resolve them in pursuit of improved measurement accuracy. All measurements presented here have been performed at very low bunch charges or with DC beams, making effects of space charge negligible.

## FACTORS AFFECTING THE MEASUREMENT

The beamlines at Cornell and ASU in which this technique has been implemented consist of a DC gun followed by at least one solenoid that can be used to focus the beam

[†]ppowusu@asu.edu

ISBN: 978-3-95450-261-5 ISSN: 2673-7000 doi: 10.18429/JACoW-NAPAC2025-TUP075



before, after, or at the pinhole. If the beam focus is at the pinhole the correlations between $x$ and $x'$ (and between $y$ and $y'$) will be minimal, showing an uncorrelated phase space. As the focus moves away from the pinhole, correlations between $x$ and $x'$ (and between $y$ and $y'$) emerge as the beam has a converging or divergent character. Despite the varying correlations, the 4D emittance in each of these scenarios should remain the same due to the linear nature of the solenoid focusing. However, this was not found to be the case. Below we detail several factors that cause this discrepancy and discuss ways of mitigating their effects. We also show that in our beamlines, the most accurate measurement of emittance can be performed when the beam is focused on the pinhole and the position-angle/momentum correlations are minimal.

### *Errors Due to Momentum Imparted by the Steering Magnet*

If only one steering magnet for each transverse direction is used to move the beam over the pinhole, it imparts a transverse momentum or an angle kick to all the electrons in the beam. This momentum is different for every beamlet that passes through the pinhole and is proportional to the distance the beam is moved on the pinhole. This momentum can be easily obtained by measuring the movement of the entire beam on the screen without the pinhole in between. For the beamline connected to the DC gun at ASU, we measured this momentum with an accuracy of ±10% relative to the true value. During the processing of the images of the various beamlets on the screen, this momentum imparted by the steering magnet must be subtracted to recover the intrinsic momentum of the electrons.

This subtraction introduces an error in the momentum measurement that is equal to the accuracy of the measurement of the momentum imparted by the steering magnet ($\sim$ 10% in the case of the ASU beamline). The larger the beam size on the pinhole the larger the momentum that the steering coil needs to impart. If this momentum is large compared to the momentum spread of the electrons in the beamlet, this error can dominate the momentum measurements. This is the case if the beam at the pinhole is converging or diverging, thus making the measurements most accurate when the beam is focused on the pinhole. This issue with the measurement was also confirmed by simulating the whole pinhole scan using General Particle Tracer (GPT) [4].

This error can be significantly mitigated by using two steering magnets to move the beam on the pinhole without giving a momentum kick.

### *Effects of Pinhole Size and Detector Resolution*

The pinhole scan technique can also be sensitive to the point spread function of the beam detector/screen used to image the beamlet transmitted through the pinhole, as well as the size of the pinhole itself. The point spread function (PSF) is the image produced by the detector in response to a point source and is often gaussian in nature. This blurs

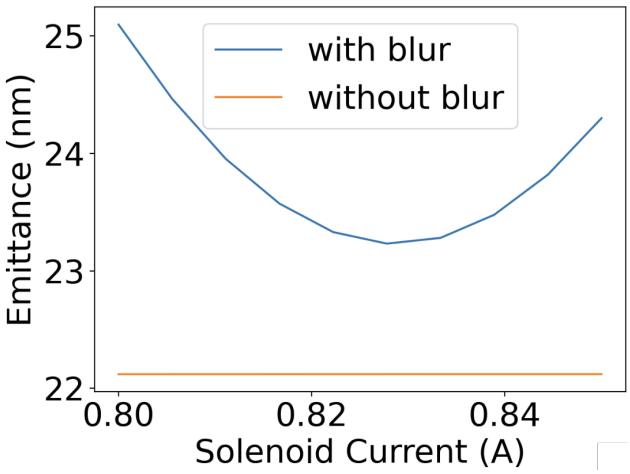


Figure 1: Emittance calculated from GPT-simulated pinhole measurement for varying solenoid focusing current. The covariance matrix of the beam used to obtain the emittance is modified with (blue) and without (orange) blurring from finite aperture size and detector point spread function.

the momentum space of the beam measured at the pinhole, which increases $\langle x'x' \rangle$ and $\langle y'y' \rangle$. The non-zero size of the pinhole also adds to the momentum blurring. Similarly, the pinhole size also applies a Gaussian blur to the position space of the beam, increasing $\langle xx \rangle$ and $\langle yy \rangle$. By convolving a Gaussian representing the aperture blur or detector PSF with a supergaussian representing a 2D projection of the 4D phase space with non-zero correlation, we can show that the off-diagonal correlation elements of the beam covariance matrix (e.g. $\langle xx' \rangle$, $\langle xy' \rangle$, $\langle xy \rangle$, etc) remain unchanged.

The contribution of pinhole and detector blurring to emittance can be expressed as,

$$\epsilon^2 = \epsilon_0^2 + \sigma_a^2 \langle x'x' \rangle + \frac{\sigma_{PSF}^2}{L^2} \langle xx \rangle + \sigma_a^2 \sigma_{PSF}^2,$$

where the $\epsilon_0$ is the true emittance, $\sigma_a$ is the rms pinhole size, $L$ is the drift length between the aperture and detector, and $\sigma_{PSF}$ is the rms size of the detector point spread function. In the Cornell beamline, $\sigma_{PSF}$ is typically large compared to $\sigma_a$, so the error of the measured emittance is dominated by the beam size $\langle xx \rangle$. Therefore, the measured emittance is smallest near the beamline setting that produces the smallest beam size at the pinhole, i.e when the beam is focused on the pinhole.

To see the effects of the pinhole size on the emittance measured by a pinhole scan, we used GPT to simulate a typical beam with an initial size of 50 µm rms and MTE of 100 meV on the photocathode. The covariance matrix is read out at the pinhole position while varying solenoid focusing currents. Gaussian blurring due to a pinhole with a diameter of 70 µm and a detector point spread function with an rms spread of 100 µm was included in the covariance matrix. Applying Eq. (2) to the modified covariance matrix, the emittance is calculated and shown in Fig. 1. We see the emittance changing by up to 10% as the solenoid focusing varies. To check that there was no error in the GPT sim-

ISBN: 978-3-95450-261-5 ISSN: 2673-7000 doi: 10.18429/JACoW-NAPAC2025-TUP075

ulation itself, we also show the emittance calculated from the original covariance matrix, which agrees with the given MTE and initial beam size. It is possible to remove these effects if the precise PSF of the detector and the RMS size of the pinhole are well known or if the PSF and the pinhole are significantly smaller than the size of the beamlets measured on the detector.

Using a smaller pinhole should help reduce the broadening of $\langle x'x' \rangle$, $\langle y'y' \rangle$, $\langle xx \rangle$ and $\langle yy \rangle$ and give more accurate emittance results. Figure 2 shows the emittance measured from a 30 µm diameter and a 10 µm diameter pinhole at different solenoid currents at the ASU beamline.

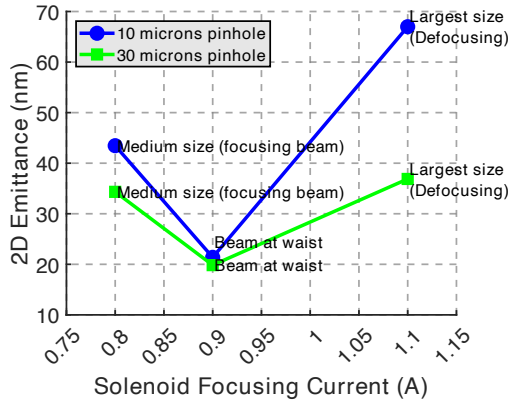


Figure 2: 2D emittance at different solenoid focusing currents for two different pinhole diameters, 10 µm (blue) and 30 µm (green). Data points correspond to relative beam sizes (medium, minimum [beam waist], and largest) illustrating the beam's focusing and defocusing effects on the emittance. The emittance measured at the beam waist agrees with the expected value for both pinhole diameters.

Both pinholes have a thickness of 100 µm, significantly larger than their diameters. For both pinholes the smallest (and the most accurate) measurement of the emittance is when the beam is focused and smallest on the pinhole as expected. However, the emittance measured using the 10 µm diameter pinhole is larger than the one measured using the 30 µm diameter pinhole at all solenoid currents. Furthermore, the difference between the measured emittance from the two pinholes increases as the size of the beam increases (away from the focus). This indicates some blurring of the momentum due to the pinhole itself. Such a blurring could be caused due to image charges of the single electrons passing through the pinholes or due to electric fields inside the pinholes due to work function variations. These effects would be more pronounced for pinholes with smaller diameters and larger thicknesses and have been observed before in other setups for measuring electron energy distributions [5]. Minimizing these effects may require a pinhole with a smaller diameter and a smaller thickness.

## EMITTANCE AND MTE MEASUREMENTS

Based on the above findings, we determined that the most accurate emittance can be measured when the beam is focused on the pinhole and correlations between the $x$ and $x'$ are minimal. At the ASU beamline we measured the emittance from a $Cs_3Sb$ photocathode on a silicon substrate using the 30 µm pinhole with the beam focused on the pinhole and extracted the MTE across various wavelengths. As shown in Fig. 3, these results are in good agreement literature [6], demonstrating that strong agreement, confirming that the errors due to the momentum subtraction, effects of the pinhole and the detector PSF are within the tolerance under the above conditions. This establishes that the pinhole scan technique can be used to perform accurate measurements of the emittance and MTE of the photocathode.

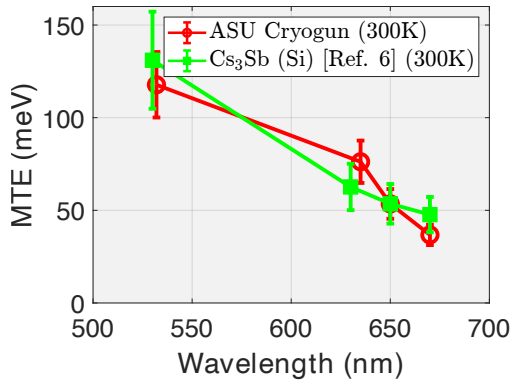


Figure 3: MTE as a function of incident laser wavelength for $Cs_3Sb$ photocathode. Measurements were performed using the refined pinhole scan technique with the ASU cryogun [3] at room temperature (300 K, red circles) compared with MTE values reported in Ref. [6] (green squares) for $Cs_3Sb$ deposited on a silicon substrate, measured using a Photoemission Electron Microscope at 300 K.

## CONCLUSION

We discussed various factors that affect the emittance and MTE measurements using the pinhole scan technique. We show that the emittance measured is most accurate when the beam waist is located at the pinhole and the position-momentum correlations are minimal. The accuracy can be significantly improved using a 2-steering magnet scheme, improving the PSF of the detector and optimizing the size of the pinhole. Finally, we show that when the beam is focused on the pinhole and when using a 30 µm pinhole we can perform reliable MTE measurements in the ASU DC gun beamline. Similar measurements have also been made at the Cornell beamlines.

## ACKNOWLEDGEMENTS

This work was supported by the U.S. National Science Foundation under Award No. PHY-1549132 the Center for Bright Beams, and the DOE under Grant Nos. DE-SC0021092 and DE-SC0020575. The work also supported in part by the U.S. Department of Energy under Contract No. DE-AC02-76SF00515 through FWP100903.

ISBN: 978-3-95450-261-5 ISSN: 2673-7000 doi: 10.18429/JACoW-NAPAC2025-TUP075

# REFERENCES


[1] M. Gordon *et al.*, "Four-dimensional emittance measurements of ultrafast electron diffraction optics corrected up to sextupole order", *Phys. Rev. Accel. Beams*, vol. 25, no. 8, p. 084001, 2022. doi:10.1103/PhysRevAccelBeams.25.084001

[2] G. Gevorkyan, C. S. Cardenas, P. Bhattacharyya, S. Karkare, and M. M. Rizi, "Phase space measurements of an electron beam using the ASU cryocooled 200 kV DC electron gun", in *Proc. IPAC'23*, Venice, Italy, May 2023, pp. 2182–2185. doi:10.18429/JACoW-IPAC2023-TUPL190

[3] P. Owusu *et al.*, "MTE measurements at the ASU cryogenically cooled DC electron gun", presented at IPAC'25, Taipei, Taiwan, Jun. 2025, paper THPM034, unpublished. https://indico.jacow.org/event/81/contributions/8255

[4] S. B. van der Geer and M. J. de Loos, "Applications of the general particle tracer code", in *Proc. PAC'97*, Vancouver, B.C., Canada, May 1997, pp. 2577–2579.

[5] S. Karkare, L. Cultrera, Y.-W. Hwang, R. Merluzzi, and I. Bazarov, "2-D energy analyzer for low energy electrons", *Rev. Sci. Instrum.*, vol. 86, no. 3, p. 033301, Mar. 2015. doi:10.1063/1.4913655

[6] A. Kachwala, P. Saha, P. Bhattacharyya, E. Montgomery, O. Chubenko, and S. Karkare, "Demonstration of thermal limit mean transverse energy from Cesium antimonide photocathodes", *Appl. Phys. Lett.*, vol. 123, no. 4, p. 044106, 2023. doi:10.1063/5.0159924